Seismic hazard from the Hispaniola subduction zone: Correction to "Historical perspective on seismic hazard to Hispaniola and the northeast Caribbean region"

Uri S. ten Brink, William H. Bakun, and Claudia H. Flores

Received 3 July 2013.

Citation: ten Brink, U. S., W. H. Bakun, and C. H. Flores (2013), Seismic hazard from the Hispaniola subduction zone: Correction to "Historical perspective on seismic hazard to Hispaniola and the northeast Caribbean region," *J. Geophys. Res. Solid Earth*, *118*, doi:10.1002/jgrb.50388.

[1] In the paper "Historical perspective on seismic hazard to Hispaniola and the northeast Caribbean region" by U. S. ten Brink et al. (*Journal of Geophysical Research*, *116*, B12318, doi:10.1029/2011JB008497, 2011), we incorrectly inferred an expected average slip of 17 m on the subduction interface rather than 1.7 m (p. 11 of 15, paragraph 33). We used this incorrect seismic slip estimate and a slip accumulation rate of 14 mm/yr to infer an incorrect recurrence interval of 1200 years for this segment of the subduction zone. Eight $M \geq 7$ earthquakes took place along this segment in the twentieth century, with two events dominating the seismic moment, the M7.7–7.9 1943 and the M7.8–8.1 4 August 1946 earthquakes [*ten Brink et al.*, 2011, Table 3]. No other comparable great historical earthquakes were felt, even though the historical record of subduction interface earthquakes in Hispaniola is likely complete for the past 500 years [*ten Brink et al.*, 2011]. *Ten Brink et al.* [2011] suggested that a 1200 year recurrence interval was consistent with these observations, but a 120 year recurrence interval is considerably shorter than the historical record. We hereafter consider the questions: Why have there been no other great earthquakes, like those in 1943 and 1946, on the subduction interface north of Hispaniola since Europeans settled in Hispaniola in 1494? What are the implications to seismic hazard from this segment of the subduction zone?

[2] Reanalyzing the 1943–1953 earthquake sequence in the region, *Dolan and Wald* [1998] noted the progression of seismic activity from east to west throughout this period. They determined the rupture area of the 1943 and 1946 earthquakes on the basis of aftershocks as 100 × 65 km and 195 × 95 km, respectively. It is thus possible that these two events, with additional smaller events during the twentieth century, have ruptured the entire 415 km long segment, defined by these earthquakes (Figure 1). *P* wave tomographic images show that this segment is the only segment with a continuous slab extending from the surface to a depth of 500 km in the northern Caribbean [*ten Brink and Villaseñor*, 2012, Figures 1c–1e]. These tomographic images were derived using the *P* wave global tomographic technique of *Bijwaard et al.* [1998], improved with additional arrival times from well-located earthquakes at both teleseismic and regional distances [*Villaseñor et al.*, 2003]. A horizontal high-velocity layer at depths <150 km underlies Haiti (Figure 2b), whereas north of Puerto Rico, the slab "is missing" at depths of 50–150 km (Figure 2f). Therefore, this 415 km long region likely defines a subduction segment.

[3] Why have there been no other great earthquakes like the 1946 earthquake in the preceding historically documented 450 years? The expected average slip during an earthquake, d, is given by

$$d = m_0/(\mu \cdot W \cdot L) \tag{1}$$

where m_0 is the seismic moment, L is the rupture length, W is the downdip rupture width, and μ is the shear rigidity. Using the Dolan and Wald's rupture length and a downdip width of 195 × 95 km for the 1946 earthquake, its estimated magnitude of 7.8–8.1 [*ten Brink et al.*, 2011, Table 3], and a shear rigidity of 30–45 GPa (typical values at depths of 20–40 km along the subduction interface) [*Bilek and Lay*, 1999], the expected median slip is 1.7 ± 0.9 m. The standard deviation is calculated by error propagation of the uncertainty in m_0 and μ. Using the estimated slip, d, the expected recurrence interval, R, of a 1946-like earthquake as a function of accumulation rate, AR, and coupling ratio, α, is

$$R = d/(\mathrm{AR} \cdot \alpha) \tag{2}$$

and is plotted in Figure 2a. The uncertainties in equation (2) include the uncertainties in the estimated slip, d, from equation (1) and the uncertainties in the accumulation rate, AR. The accumulation rate can vary from 4 to 6 mm/yr, the perpendicular rate of plate convergence, to 14 mm/yr, the plate motion rate resolved into the oblique slip direction of the 1946 earthquake [*Dolan and Wald*, 1998]. It is difficult to estimate the coupling ratio, α, from the one period of earthquakes (the twentieth century); however, *Manaker et al.* [2008] suggested coupling of 0.45 ± 0.26 for this segment based on geodetic modeling.

[4] A recurrence interval longer than the historical record (≥450 year) is predicted for an expected median slip of 1.7 m and an accumulation rate of 14 mm/yr, if the coupling is low ($\alpha \leq 0.28$) (Figure 2a). On the other hand, the coupling is ≤0.95 for an accumulation rate that assumes a trench-perpendicular slip (4 mm/yr). The grey area in Figure 2a marks

©2013. American Geophysical Union. All Rights Reserved.
2169-9313/13/10.1002/jgrb.50388

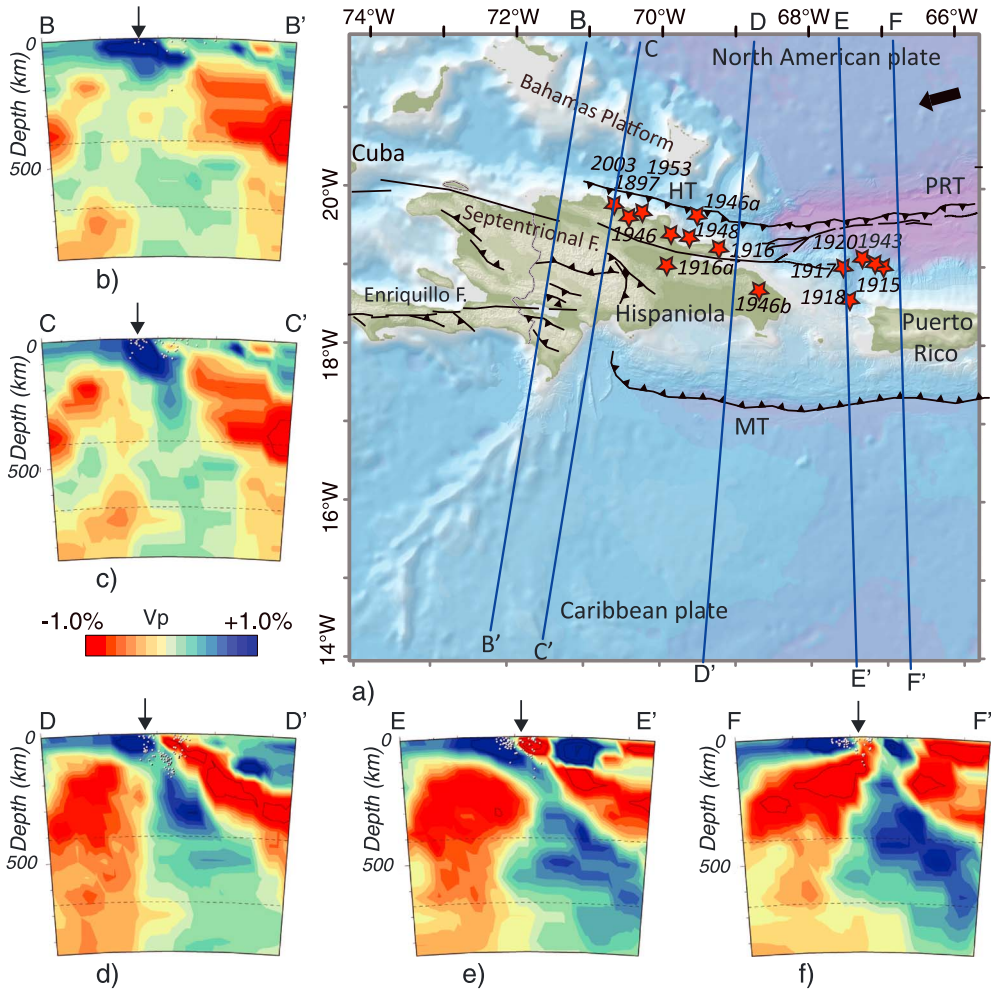

Figure 1. (a) Locations of twentieth century earthquakes, as listed in *ten Brink et al.* [2011, Table 3] plus the *M*6.4 2003 earthquake. HT: Hispaniola Trench; PRT: Puerto Rico Trench; MT: Muertos Trough. Barbed lines: Thrust faults. Thin lines: Strike-slip faults. Blue lines: Locations of the tomographic profiles in Figures 1b–1f. (b–f) *P* wave tomographic profiles in the vicinity of Hispaniola (from *ten Brink and Villaseñor* [2012]). Small arrows mark the locations of the north shore of the islands and of the 1918 epicenter. Note that twentieth century earthquakes are limited to the 415 km long region showing a continuously dipping slab (profiles in Figures 1b–1e). Velocity anomalies are relative to the global 1-D reference model ak-135 [*Kennett et al.*, 1995].

the uncertainty in the 450 year contour of recurrence interval arising from the uncertainty in the calculated seismic slip ($d = 1.7 \pm 0.9$ m). The contour of the negative standard deviation represents combinations of low m_0 and high μ, and the positive represents high m_0 and low μ. If either the largest slip (2.6 m/yr) or the median slip (1.7 m/yr) is valid and if the *Manaker et al.* [2008] range of coupling is valid, recurrence intervals longer than the historical record can be expected for an oblique slip similar to the 1946 earthquake rupture. However, if the smallest slip is valid and if Manaker's range of coupling is valid, then the accumulation rate must be ≤0.95 mm/yr; in other words, the rupture direction is expected to be less oblique than the 1946 slip azimuth.

[5] Instead of using the 1946 earthquake rupture parameters as representatives of earthquakes along this segment, we can use rupture parameters from global compilations of thrust earthquakes [e.g., *Blaser et al.*, 2010]. Oblique convergence takes place in many subduction zones [e.g., *McCaffrey*, 1994], and we contend that the subduction segment north of Hispaniola is not unique in this respect. The combined twentieth century earthquakes moment for this segment ranges between 1.87×10^{21} and 3.46×10^{21} N m depending on the magnitude of the 1943 and 1946 earthquakes and is the equivalent of a single *M*8.1–8.3 earthquake. Using the *Blaser et al.* [2010] empirical relationships between earthquake magnitude and the length and downdip rupture width of thrust earthquakes ($\log_{10}L = -2.37 + 0.57 * M$; $\log_{10}W = -1.86 + 0.46 * M$), rupture length and width of 177–230 km and 73–91 km, respectively, are expected for a single earthquake with a magnitude of 8.1–8.3. According to equation (1), the expected seismic slip and its standard deviation is $d = 4.3 \pm 1.7$ m. The uncertainty in μ is 30–45 GPa, as indicated above. The standard deviation in the seismic slip is calculated using propagation of errors for the uncertainties in m_0, L, W, and μ.

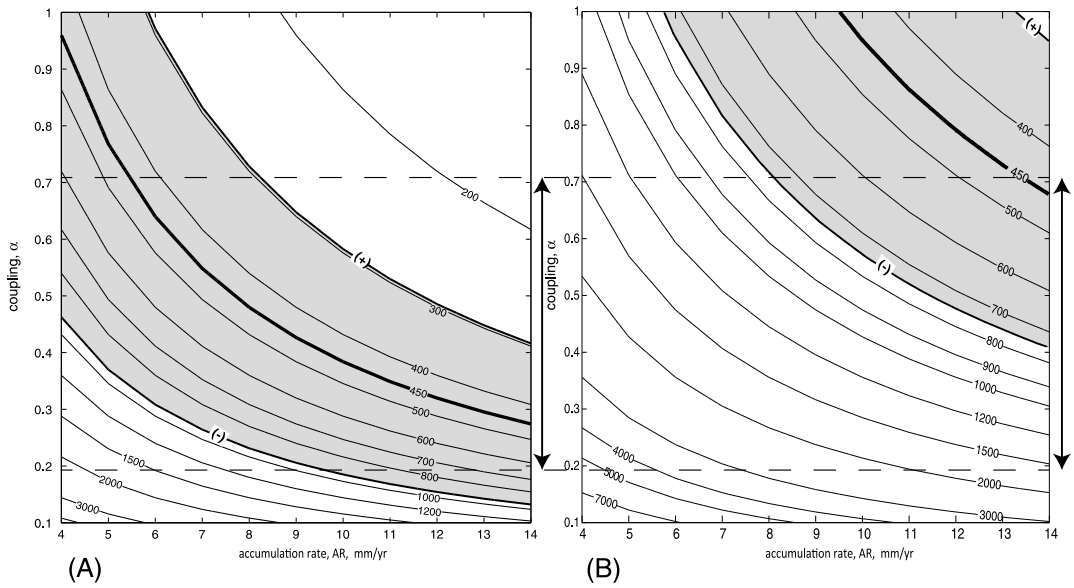

Figure 2. Recurrence interval, R (thin contours), as a function of accumulation rate and seismic coupling (a) for an earthquake rupture similar to the 4 August 1946 earthquake, the largest known earthquake along this subduction segment, and (b) for an earthquake with the total moment of all large earthquakes that took place in this subduction zone in the twentieth century. The rupture area in Figure 2a is from *Dolan and Wald* [1998] for the 1946 earthquake, and the rupture area in Figure 2b is based on the *Blaser et al.* [2010] scaling relationship between magnitude and rupture length and width (see text). The 450 year recurrence interval is highlighted (heavy line) because the historic record does not indicate a large ($M > 7.5$) earthquake in the 450 years preceding the 1943 and 1946 earthquakes. Contours marked minus and plus are the negative and positive standard deviations of the 450 year recurrence interval, given the uncertainties in rupture area, earthquake magnitudes of the 1943 and 1946 earthquakes, and shear rigidity (see text for further details). Double-sided arrows and dashed lines indicate the range of coupling derived from the geodetic model of *Manaker et al.* [2008].

[6] A recurrence interval longer than the historical record (≥450 years) is predicted for an expected median slip of 4.3 m, an accumulation rate of 14 mm/yr, and coupling of 0.68, which is close to the uppermost coupling estimate of *Manaker et al.* [2008](Figure 2b). If Manaker's average coupling estimate (0.45) represents the coupling ratio on the subduction interface, then the earthquake recurrence interval is expected to be ≥700 years for all accumulation rates and for the median earthquake magnitudes, rupture area, and μ. The grey area in Figure 2b marks the uncertainty in the 450 year contour of recurrence interval arising from the uncertainty in the calculated seismic slip ($d = 4.3 \pm 1.7$ m). The largest slip is a combination of the largest moment and the smallest rupture area and shear rigidity, and the opposite applies to the smallest slip. If the largest slip is valid, $\alpha \sim 1$, even for AR = 13–14 mm/yr. If the smallest slip is valid, accumulation rates of ≤14 mm/yr fall within the estimated coupling by *Manaker et al.* [2008].

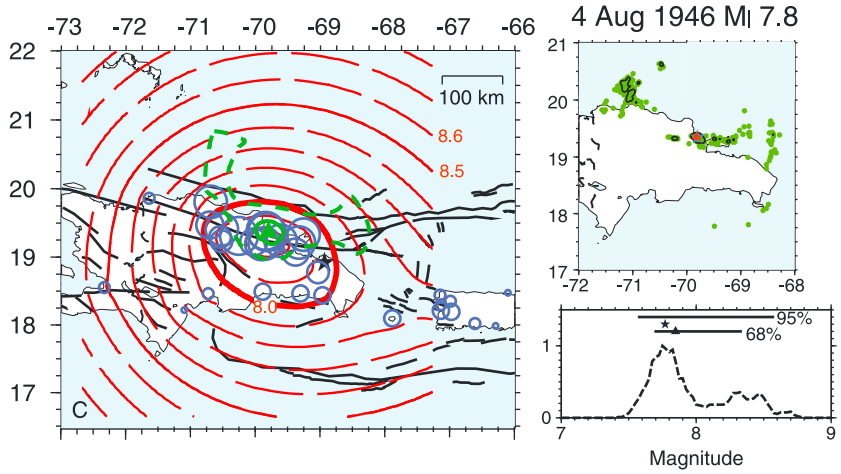

Figure 3. A corrected Figure 4c from *ten Brink et al.* [2011].

[7] As shown in Figure 2, in all cases, reasonable parameter combinations (magnitude, rupture area, shear rigidity, accumulation rate, and coupling) can be found that result in recurrence intervals that are consistent with the absence of additional large historical subduction events prior to the twentieth century series of earthquakes. In all but one case, an accumulation rate of 14 mm/yr (the oblique component similar to the slip azimuth during the 1946 earthquake) and the range of coupling values estimated by *Manaker et al*. [2008] give recurrence intervals ≥450 years, in accord with the historical record analyzed in *ten Brink et al*. [2011]. An accumulation rate of 4 mm/yr (the perpendicular component of plate convergence) and Manaker's coupling range give recurrence intervals >450 years for the entire ranges of all the parameters.

[8] It is also possible, however, that a uniformly repeating recurrence model does not describe the seismic behavior of this segment of the subduction zone, and therefore, the seismic hazard in this region cannot be completely evaluated from information based on a single cycle of earthquake ruptures [e.g., *Bakun et al*., 2005; *Shelly*, 2010]. An alternative assumption is that earthquakes within a certain tectonic zone result from a random (Poisson) process. Two $M > 7\frac{1}{2}$ earthquakes have occurred in the 415 km long subduction zone north of Hispaniola during the past 450 years. The Poisson rate, r, for this zone is therefore $2/450 = 0.0044$, and the probability that at least one more $M > 7\frac{1}{2}$ earthquake will occur on this segment in the next $t = 50$ years is

$$P = 1 - \exp(-r \cdot t) \quad [\textit{Rong et al.}, 2003] \tag{3}$$

Hence, if the earthquake distribution on the subduction zone north of Hispaniola is random with time, the probability for another $M > 7\frac{1}{2}$ earthquake to occur there within the next 50 years is <20%.

[9] We can also use the global empirical relationship between magnitude and rupture length of thrust earthquakes [*Blaser et al*., 2010] to estimate the expected maximum magnitude earthquake in this subduction zone. A rupture of the 415 km long subduction segment (Figure 1) during a single event would generate an M8.75 earthquake. The moment of such an earthquake would be almost 5 times the combined seismic moment of the twentieth century earthquakes. A single rupture of this segment does not have to occur every earthquake cycle, as was observed in the 2011 Tohoku-Oki earthquake and the preceding earthquakes on the Japan Trench.

[10] We also regret an error in Figure 4c from *ten Brink et al*. [2011] that occurred during figure production. The blue circles, the green triangle, and the dashed green lines were shifted north about 40 km from their proper locations, and the green circle around the green triangle was painted in red. The corrected figure is shown here (Figure 3).

[11] **Acknowledgments.** We are indebted to Gavin Hayes for pointing out the error in our calculation and for proposing and helping with the preparation of Figure 2. We thank Eric Geist for discussions regarding Poisson distribution. Antonio Villaseñor provided the tomographic cross sections in Figure 1. Gavin Hayes, Daniel McNamara, and Robert Nowack (Editor) provided helpful reviews.

References

Bakun, W. H., et al. (2005), Implications for prediction and hazard assessment from the 2004 Parkfield earthquake, *Nature*, *437*, 969–974.

Bijwaard, H., W. Spakman, and E. R. Engdahl (1998), Closing the gap between regional and global travel time tomography, *J. Geophys. Res.*, *103*, 30,055–30,078.

Bilek, S. L., and T. Lay (1999), Rigidity variations with depth along interpolate megathrust faults in subduction zones, *Nature*, *400*, 443–446.

Blaser, L., F. Krüger, M. Ohrnberger, and F. Scherbaum (2010), Scaling relations of earthquake source parameter estimates with special focus on subduction environment, *Bull. Seismol. Soc. Am.*, *100*, 2914–2926.

Dolan, J. F., and D. J. Wald (1998), The 1943–1953 north-central Caribbean earthquakes: Active tectonic setting, seismic hazards, and implications for Caribbean–North America plate motion, *Geol. Soc. Am. Spec. Publ.*, *326*, 143–169.

Kennett, B., E. Engdahl, and R. Buland (1995), Constraints on seismic velocities in the Earth from traveltimes, *Geophys. J. Int.*, *122*, 108–124.

Manaker, D. M., E. Calais, A. M. Freed, S. T. Ali, P. Przybylski, G. Mattioli, P. Jansma, C. Prépetit, and J. B. de Chabalier (2008), Interseismic plate coupling and strain partitioning in the northeastern Caribbean, *Geophys. J. Int.*, *174*, 889–903.

McCaffrey, R. (1994), Global variability in subduction thrust zone-forearc systems, *Pure Appl. Geophys.*, *142*, 173–224.

Rong, Y., D. D. Jackson, and Y. Y. Kagan (2003), Seismic gaps and earthquakes, *J. Geophys. Res.*, *108*, B05S08, doi:10.1029/2002JB002334s.

Shelly, D. R. (2010), Periodic, chaotic, and doubled earthquake recurrence intervals on the Deep San Andreas Fault, *Science*, *328*, 1385–1388.

ten Brink, U. S., and A. Villaseñor (2012), Caribbean plate tectonics from seismic tomography, Abstract T33H-02 presented at 2012 Fall Meeting, AGU, San Francisco, Calif., 3–7 Dec.

ten Brink, U. S., W. H. Bakun, and C. H. Flores (2011), Historic perspective on seismic hazard to Hispaniola and the northeast Caribbean region, *J. Geophys. Res.*, *116*, B12318, doi:10.1029/2011JB008497.

Villaseñor, A., W. Spakman, and E. R. Engdahl (2003), Influence of regional travel times in global tomographic models, *Geophys. Res. Abstr.*, EGS-AGU-EUG Joint Assembly, 2003, 1, 8614.